Marine Chemistry 124 (2011) 125–133

Contents lists available at ScienceDirect

Marine Chemistry

journal homepage: www.elsevier.com/locate/marchem

Assessing the dynamics of chromophoric dissolved organic matter in a subtropical estuary using parallel factor analysis

Weidong Guo [a], Liyang Yang [a], Huasheng Hong [a,*], Colin A. Stedmon [b], Fuli Wang [a], Jing Xu [a], Yuyuan Xie [a]

[a] State Key Laboratory of Marine Environmental Science, Xiamen University, Xiamen, Fujian 361005, China
[b] Department of Marine Ecology, National Environmental Research Institute, Aarhus University, Frederiksborgvej 399, 4000 Roskilde, Denmark

ARTICLE INFO

Article history:
Received 30 April 2010
Received in revised form 29 November 2010
Accepted 12 January 2011
Available online 22 January 2011

Keywords:
Chromophoric dissolved organic matter
Excitation emission matrix fluorescence spectroscopy
Parallel factor analysis
Jiulong Estuary

ABSTRACT

The spatial and temporal dynamics of chromophoric dissolved organic matter (CDOM) were studied using excitation emission matrix fluorescence spectroscopy (EEMs) and parallel factor analysis (PARAFAC) during five cruises in the subtropical Jiulong Estuary from August 2008 to June 2009. Two humic-like (C1 and C3), one tryptophan-like (C4) and one possible protein-like (C2) component was identified by PARAFAC and their behavior in the river–estuary–coastal interface was evaluated. The spatial distributions of the maximum fluorescence (F_{max}) for the fluorescent components showed a remarkable loss in the upper estuary. The following significant addition of all components in the low salinity turbidity maximum zone suggested the inputs from riverine source, sediment resuspension and the surrounding mangrove ecosystem. C1, C2 and C3 showed conservative behavior in the middle and lower estuary indicated by the linear relationship between their fluorescence intensities and salinity in the five cruises. However, the tryptophan-like C4 received widespread additions (likely from autochthonous production) in the estuary. Although the humic-like C1 and C3 showed no significant variation in the estuary–coastal interface, C2 and C4 decreased more rapidly beyond this interface, indicating the significant influence of coastal current to this estuarine environment. The seasonal variation of tryptophan-like C4 was characterized by higher F_{max} values in the upper to middle estuary in the dry season, which is in contrast to that of the humic-like C3. Correlation analysis with DOC showed that the fluorescence intensity of C1 (or C2 and C3) was suitable for tracing DOC dynamics in this estuary. These results indicated different mixing behavior and temporal variability for different fluorescent components in this dynamic estuarine environment.

1. Introduction

Chromophoric dissolved organic matter (CDOM), the light-absorbing fraction of dissolved organic matter (DOM), is a complex mixture of organic compounds that originates from a wide range of sources and is subjected to removal and diagenetic processes (Hansell and Carlson, 2002; Coble, 2007). CDOM can affect the aquatic primary production by absorbing photosynthetically active radiation and protect organism from harmful ultraviolet radiation (Foden et al., 2008; Zepp et al., 2008). In addition, CDOM interacts with trace metals to form organometal complexes (Yamashita and Jaffé, 2008) and releases trace gases (e.g., CO and CO_2), nutrients and low molecular weight organic compounds through biological and photochemical degradation (Bushaw et al., 1996; Moran and Zepp, 1997; Kieber et al., 1990). CDOM is also used to discriminate and trace water masses (Coble et al., 1998; Hong et al., 2005) and to estimate the concentrations of dissolved organic carbon (DOC) and specific constituents (e.g., amino acids and lignin) (Yamashita and Tanoue, 2003; Spencer et al., 2009).

Since the 1990s, excitation emission matrix fluorescence spectroscopy (EEMs) has been widely used to characterize the sources, transformation and behavior of CDOM in aquatic environments (e.g., Coble, 1996, 2007). Generally, two major types of fluorescent groups have been identified in natural waters: humic-like and protein-like. Recently, EEMs were combined with parallel factor analysis (PARAFAC) to identify individual fluorescent components and trace their sources and dynamics (Stedmon et al., 2003). This technique provides a powerful tool to shed light on the biogeochemical cycles of DOM, a large active carbon pool that is currently poorly characterized. In particular, the conservative or non-conservative behavior of different fluorescent components have been found during the mixing of freshwater and seawater in estuaries, the dynamic land-ocean interaction zone (Stedmon and Markager, 2005; Yamashita et al., 2008; Kowalczuk et al., 2009; Fellman et al., 2010).

Although there are an increasing number of studies on CDOM using EEMs-PARAFAC in estuarine environments (Stedmon et al., 2003; Stedmon and Markager, 2005; Yamashita et al., 2008; Kowalczuk et al., 2009; Fellman et al., 2010), there is still little

* Corresponding author.
E-mail address: hshong@xmu.edu.cn (H. Hong).

0304-4203/$ – see front matter © 2011 Elsevier B.V. All rights reserved.
doi:10.1016/j.marchem.2011.01.003

information concerning on the dynamics of CDOM fluorescent components in a whole estuarine system (i.e., from the watershed–estuary interface to the estuary–coastal interface). These two interfaces are very dynamic due to the ionic strength change, the occurrence of turbidity maximum zone and sediment resuspension in the watershed–estuary interface, and the interaction between estuarine plume and coastal currents in the estuary–coastal interface. In addition, anthropogenic activities such as sewage discharge can affect the DOM concentration, chemical composition and reactivity, especially in densely populated rivers and their estuaries (Baker, 2001; Abril et al., 2002; Hong et al., 2005; Spencer et al., 2007). Some estuaries also have severe eutrophication problems and frequent harmful algal bloom events due to a large amount of nutrient input, which can also influence the estuarine DOM dynamics (e.g., Gors et al., 2007; Sharp et al., 2009).

The Jiulong Estuary is a shallow subtropical estuary with a high turbidity in the low salinity region and is influenced by East Asian Monsoon and typhoon-associated extreme events. The dissolved nutrient concentrations (N and P) have increased by two to three times in the recent two decades (Chen et al., 1985; Zhai et al., unpublished data). Multiple tributary inputs at its head and strong monsoon-driven coastal currents near its mouth make the interface processes very complicated at both sides of the estuary. Five comprehensive physical, chemical, biological and sedimentological investigations were carried out in this estuary during 2008–2009, trying to understand estuarine biogeochemical processes under the context of global change and anthropogenic disturbance. In this study, we aimed to trace the dynamics of DOM fluorescent components identified by PARAFAC, to provide an insight into the variability of DOM in this estuary, with emphasis on the interface processes and the seasonal variability based on the five cruises from August 2008 to June 2009.

2. Materials and methods

2.1. Study area

The Jiulong Estuary is a subtropical estuary in southeastern China, on the west coast of the Taiwan Straits (Fig. 1). The mean annual

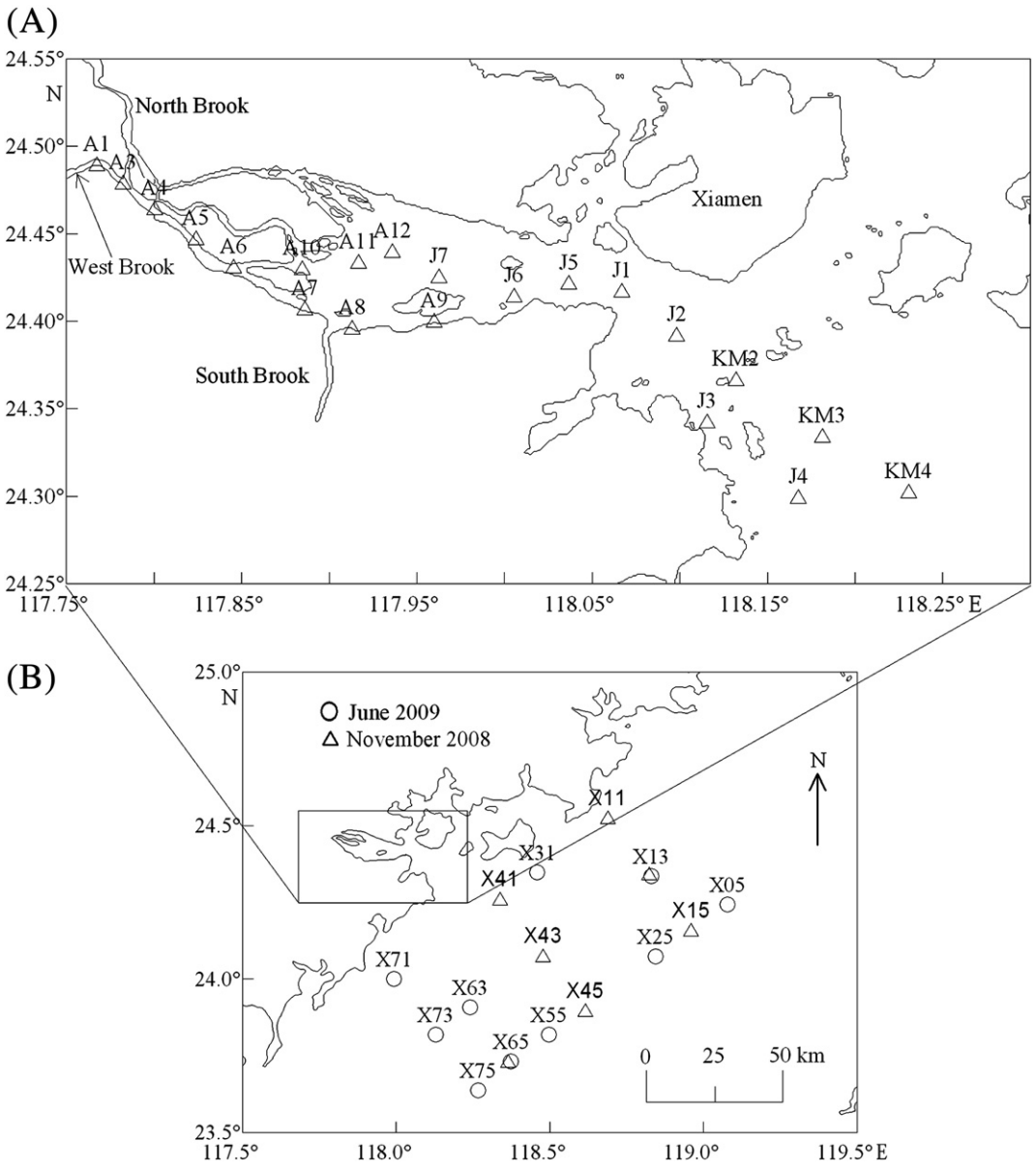

Fig. 1. Study area and sampling station. (A) Samples were collected throughout the estuary and along the salinity gradient from August 2008 to June 2009, although some stations (J (3–5), J7, KM(2–4)) were not sampled in some cruises. (B) The sampling area was further extended to the adjacent coastal ocean in November 2008 and June 2009.

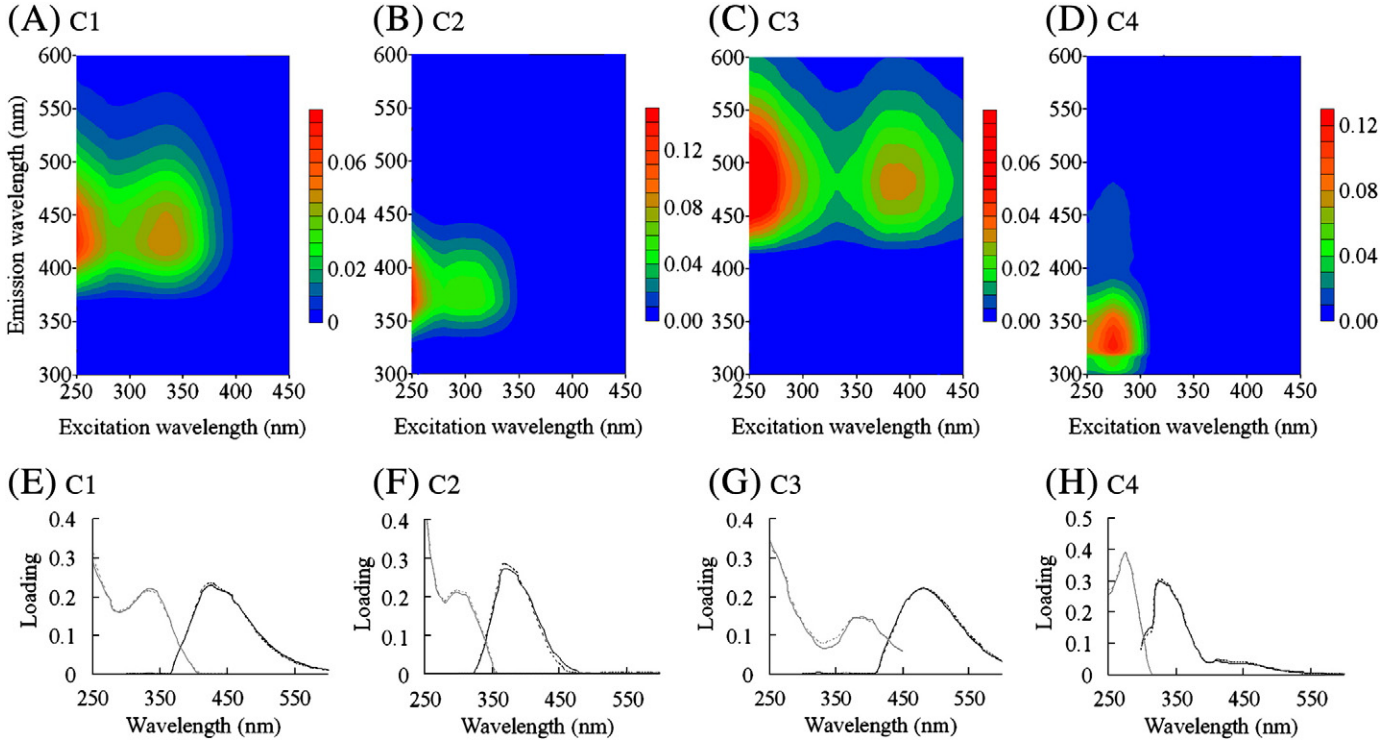

Fig. 2. The spectral characteristics of the four fluorescent components identified by PARAFAC. Graphs (A–D) show the EEMs contours of individual components; graphs (E–H) show the excitation (gray lines) and emission (black lines) loadings of the components, dashed lines and solid lines show the similarity of two independent, four-component PARAFAC models on two random halves of the whole data (i.e., split-half validation).

precipitation and water temperature are 1772 mm and 20.9 °C. The climate of the estuary and its watershed are influenced by the East Asian Monsoon; as tropical storms (typhoons) strike this area several times a year, they are accompanied with extremely high precipitation events over a short period of time. The length of the estuary is 21 km and the average width is 6.5 km. The tides of the estuary are semidiurnal with a mean tidal range of 2.7–4 m from the upper to the lower estuary. Some nutrients are very abundant in the estuary, especially in the low and middle salinity regions (Yang and Hu, 1997). The concentrations of nitrate and silicate are >100–240 μM and 200–300 μM at the freshwater endmember (Zhai et al., unpublished data; Yang and Hu, 1997). The concentration of total suspended matter is highest in the freshwater zone and decreases rapidly in the low salinity zone (Yang and Hu, 1997). The coastlines of the lower salinity part of the estuary are bordered by mangroves. The Jiulong River consists of three tributaries, namely North Brook, West Brook and South Brook, with a drainage area of 11,909 km^2. The North Brook is the main stream and converges with the West Brook at the head of the estuary, while the South Brook is a small brook entering the middle estuary. The combined mean annual runoff of the North and West Brooks into the estuary is 123×10^8 m^3, mostly discharged (~74%) in the wet season from April to September.

2.2. Sample collection

Surface and bottom water samples were collected using Niskin bottles during five cruises throughout the estuary in August, November 2008 and February, May, June 2009 (Fig. 1A). Most of the sampling stations were located in the main channel of freshwater outflow (i.e., along the south bank), to trace the mixing of freshwater and seawater. Generally, water samples were collected from station A1 to KM4. However, the sampling plans were designed to cover a wide range of salinity and not all the stations were sampled in every cruise. In November and June, samples from the coastal ocean were also collected (Fig. 1B). Salinity was measured using a SBE917 Plus self-contained CTD (conductivity–temperature–depth) profiling system (Sea-Bird Electronics Inc., USA) and a wide range of salinities from 0 to 34 were covered in this study. The sample size was 38, 73, 64, 26 and 56 in August, November 2008 and February, May, June 2009, respectively. Samples were filtered through precombusted (500 °C for 5 h) GF/F filters and then acidified with HCl for DOC and total dissolved nitrogen (TDN) measurements. Samples for fluorescence measurements were filtered through acid-rinsed 0.2 μm Millipore polycarbonate filters.

Table 1
Spectral characteristics of the four fluorescent components identified by the PARAFAC model in this study, compared with those previously identified. Excitation/emission maxima (nm) are presented, with secondary excitation maxima in brackets.

Components in this study	Coble (1996), Coble et al. (1998)	Stedmon et al. (2003)	Stedmon and Markager (2005)	Yamashita et al. (2008)	Murphy et al. (2006)
C1: ≤250 (335)/428	Peak A: 260/380–460, Peak M: 290–312/370–420	C2: <240/416, C4: 325 (250)/416	C2: <250 (305)/412 C5: 325/428	\	C8: 250 (380)/416
C2: ≤250 (300)/368	Peak N: 280/370	C5: 280 (<240)/368	\	C5: 285/362	C4: 250 (320)/370
C3: ≤250 (380)/484	Peak A: 260/380–460, Peak C: 320–360/420–480	C3: 270 (360)/478	C1: <250/448	C3: 390 (275)/479	C3: 260 (370)/490
C4: 275/328	Peak T: 275/340	\	C7: 280/344	\	C7: 240 (300)/338

2.3. DOC, TDN and chlorophyll a measurements

DOC was measured for all cruises, while TDN was only measured from August, 2008 to February, 2009. DOC and TDN were measured with a Multi N/C 3100 TOC-TN analyzer (Analytik Jena, Germany). Each sample was analyzed at least twice; and when the variation coefficient was >2%, more measurements were carried out. Samples were acidified and purged with oxygen for 8 min to remove the inorganic carbon before high temperature catalytic oxidation. Potassium hydrogen phthalate and potassium nitrate solutions were used as standards for DOC and TDN calibration, respectively. The accuracy was verified daily with Low Carbon Water and Deep Sea Water provided by University of Miami (D. A. Hansell). Chlorophyll *a* was determined by measuring fluorescence at the excitation and emission wavelengths of 430 nm and 670 nm, using a Shimadzu (RF-5301PC) spectrofluorometer (Ou et al., 2006).

2.4. EEMs analysis and PARAFAC modeling

EEMs were measured using a Cary Eclipse fluorescence spectrophotometer (Varian, Australia) by scanning a series of emission spectra from 230 to 600 nm (every 2 nm) while exciting at 200–450 nm (every 5 nm). The fluorescence spectra were corrected following the instrument's manual. Samples were not corrected for inner filter effects because of low CDOM concentrations (a_{350}: 0.97 ± 0.74 m^{-1}, unpublished data; Han and Guo, 2008). The sample EEMs were Raman calibrated (Lawaetz and Stedmon, 2009) and subtracted by a Raman normalized Milli-Q water EEMs which was scanned on the same day. However, the fluorescence at excitation wavelengths below 250 nm and emission wavelengths below 300 nm were not used for further analysis to avoid the interference of noise signals (Stedmon and Markager, 2005). Then, the EEMs were modeled by PARAFAC using MATLAB 7.5 and "the N-way toolbox for MATLAB" (Andersson and Bro, 2000; Stedmon and Bro, 2008). Split-half validation was used to determine the number of components (Fig. 2; Stedmon and Bro, 2008). PARAFAC analysis decomposed the EEMs into individual components and the fluorescence of each component was represented by the maximum fluorescence F_{max} (RU, i.e., Raman units) (Stedmon and Markager, 2005; Kowalczuk et al., 2009).

3. Results and discussion

3.1. Fluorescent component characteristics

Four fluorescent components were identified using PARAFAC (Fig. 2; Table 1): two humic-like components (C1 and C3), one tryptophan-like component (C4) and one possible protein-like component (C2). C1 is found both in freshwater and seawater (Coble, 1996; Baker, 2001; Stedmon et al., 2003; Stedmon and Markager, 2005). Given that the level of this component was much higher in freshwater than in coastal ocean and also elevated in the wet season (see the following discussion), C1 represented mainly terrestrial humic-like substances in this study. C2 might be peak N or a combination of peak N and tryptophan-like material (Coble et al., 1998; Stedmon et al., 2003; Yamashita et al., 2008). But some studies suggest a similar component to be polyaromatic hydrocarbons (i.e., PAHs, Murphy et al., 2006) or humic-like substances (e.g., Cory and McKnight, 2005; Fellman et al., 2010). However, the estuarine distribution of PAHs (X. H., Wang, unpublished data) was totally different from that of C2 in Jiulong Estuary. A similar component in Jiulong River watershed is correlated with tryptophan-like component ($r = 0.77$) much more closely than with humic-like component ($r = 0.33$–0.50, Hong et al., in press). Hence, it appears to be more likely protein-like in the study area but derived from freshwater

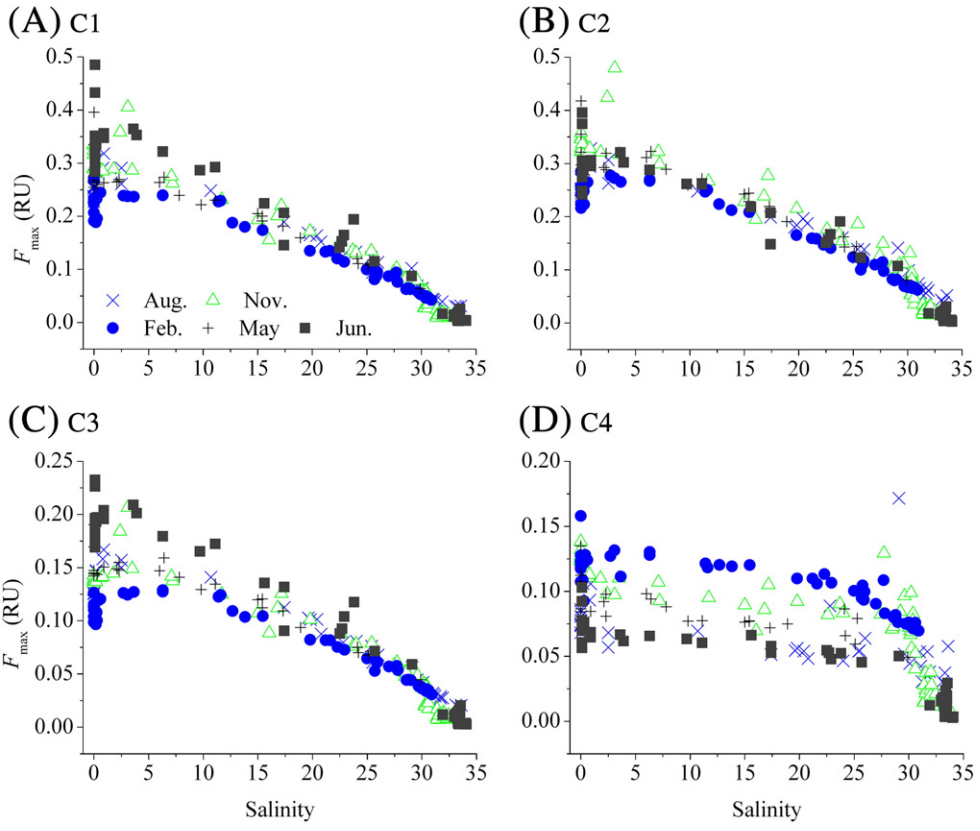

Fig. 3. The relationships between F_{max} of individual components C(1–4) and salinity (graphs (A–D)), refer to graph A for the corresponding months to different symbols.

sources considering the much higher abundance in freshwater than in seawater. C3 resembled a combination of peak A and peak C (Coble, 1996). Stedmon and Markager (2005) find two similar components of either terrestrial or autochthonous sources, with higher concentrations in freshwater than those in marine water. Yamashita et al. (2008) suggest that it can be of terrestrial origin and produced through biogeochemical processing of terrestrial particulate organic matter. The spectral characteristic of C4 resembled that of tryptophan (excitation and emission maxima (nm): 275-280/340-354, Yamashita and Tanoue, 2003). The tryptophan-like component can be derived from both allochthonous and autochthonous sources (Stedmon and Markager, 2005; Yamashita et al., 2008). In this study, C4 likely received additions from in situ production within the estuary, in addition to the freshwater input.

3.2. Behavior during estuarine mixing

3.2.1. C1-C3 components

The relationship between F_{max} values for PARAFAC components and salinity can be used to determine conservative or non-conservative behavior of different DOM fractions during mixing of freshwater and seawater. The estuarine mixing behavior of each component was similar between the surface and the bottom waters, likely due to the shallow water depth (<10 m in average within the estuarine mouth) and short water exchange time (~2 days) of the estuary (Hong and Cao, 2000). Therefore, all the mixing plots below were a combination of both the surface and the bottom. F_{max} of C1, C2 and C3 decreased overall with increasing salinity, especially in the middle and high salinity regions (almost linearly, Fig. 3). This suggests these components originated primarily from fluvial inputs and behaved conservatively in the middle and lower estuary. This was perhaps expected for C3 which is representative of terrestrial humic-like material (e.g., Yamashita et al., 2008). Autochthonous production within the estuary did not influence evidently the estuarine behavior of C1, although marine humic-like materials (i.e., peak M) might contribute somewhat to fluorescence at these wavelengths. The strong correlations to salinity and intercorrelation between C1 and C3 (Fig. 4) suggested that they were largely derived from fluvial input (i.e., terrestrially-derived).

In the low salinity zone, these three components generally showed non-conservative behavior (Fig. 3). Here we just take C1 as an example, as both C2 and C3 covaried with C1 in the low and middle salinity zone (Fig. 4A, B). C1 received an overall addition from A5 to A7 in June (Fig. 5A), indicating the contribution from additional sources such as the degradation of organic matter from resuspended and/or sinking particles as well as vertical diffusion of CDOM from pore water. Higher concentration of pCO_2 in this region likely indicates the occurrence of the transformation of particulate organic matter (W. D. Zhai, unpublished data). CDOM in the sediment pore water also has a high concentration in this area (Cheng et al., 2008). In November, much higher F_{max} values of C1 occurred in A8 which is located just downstream to the mouth of the South Brook (Fig. 5B), highlighting the importance of terrestrial DOM inputs from this tributary. In addition, this region is surrounded by mangrove wetlands and may receive significant inputs from the intertidal system. The significant addition of DOM from mangrove wetlands has been found in previous studies (e.g., Jaffé et al., 2004) and a recent study confirms the production of CDOM from mangrove litters (Shank et al., 2010).

3.2.2. C4 component

F_{max} of the tryptophan-like C4 changed greatly in freshwater (Fig. 5C, D) and declined in high salinity waters (salinities>25–30 in different cruises, Fig. 3D), and it did not undergo conservative mixing (i.e., decrease with increasing salinity) in the low or middle salinity region (Fig. 3D). Instead, this component likely received widespread additions (e.g., in situ production) in the estuary (Fig. 3D), which was

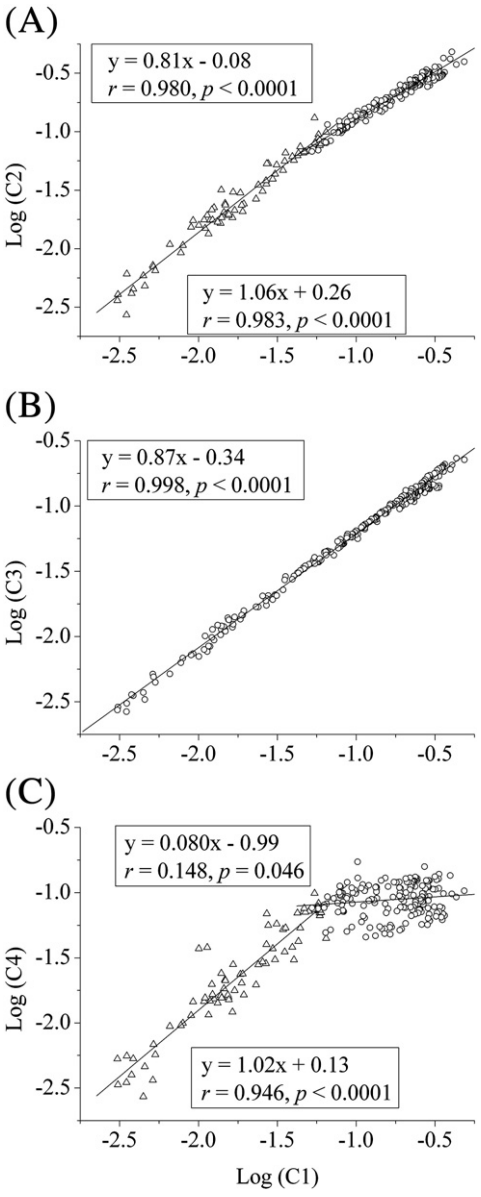

Fig. 4. Non-linear regressions between F_{max} of paired components: (A) C2 versus C1; (B) C3 versus C1; (C) C4 versus C1. Samples were separated into two subsets (with salinity >30 and ≤30) in graphs A and C.

further confirmed by the fact that no correlation occurred between log (C4) and log (C1) in Jiulong estuary with salinity <30 (Fig. 4C). This indicated the decoupling behavior and different source for humic-like and tryptophan-like components in the Jiulong Estuary. The decoupling would cause an increase in the percent of C4 in the total fluorescence with increasing salinity, which might affect the associated bioavailability and hence the biogeochemical role of DOM. For example, the bioavailability of DOM is positively correlated with the percent of protein-like components (Fellman et al., 2010, and references therein).

3.2.3. DOC and TDN

In this study, DOC varied both spatially and temporally, ranging from 0.63 mg L^{-1} to 2.89 mg L^{-1} (Fig. 6A). The mean value of DOC in the freshwater endmember of Jiulong Estuary was 1.89 ± 0.33 mg L^{-1}. Comparing with other rivers in this region, it was slightly higher than that in the Changjiang River (~1.3 mg L^{-1}, Wu et al., 2007) but lower than that in the upper reach of the Zhujiang Estuary (3.66 ± 1.16 mg L^{-1}, He et al., 2010). In the low salinity zone, DOC was not conservative, likely due to

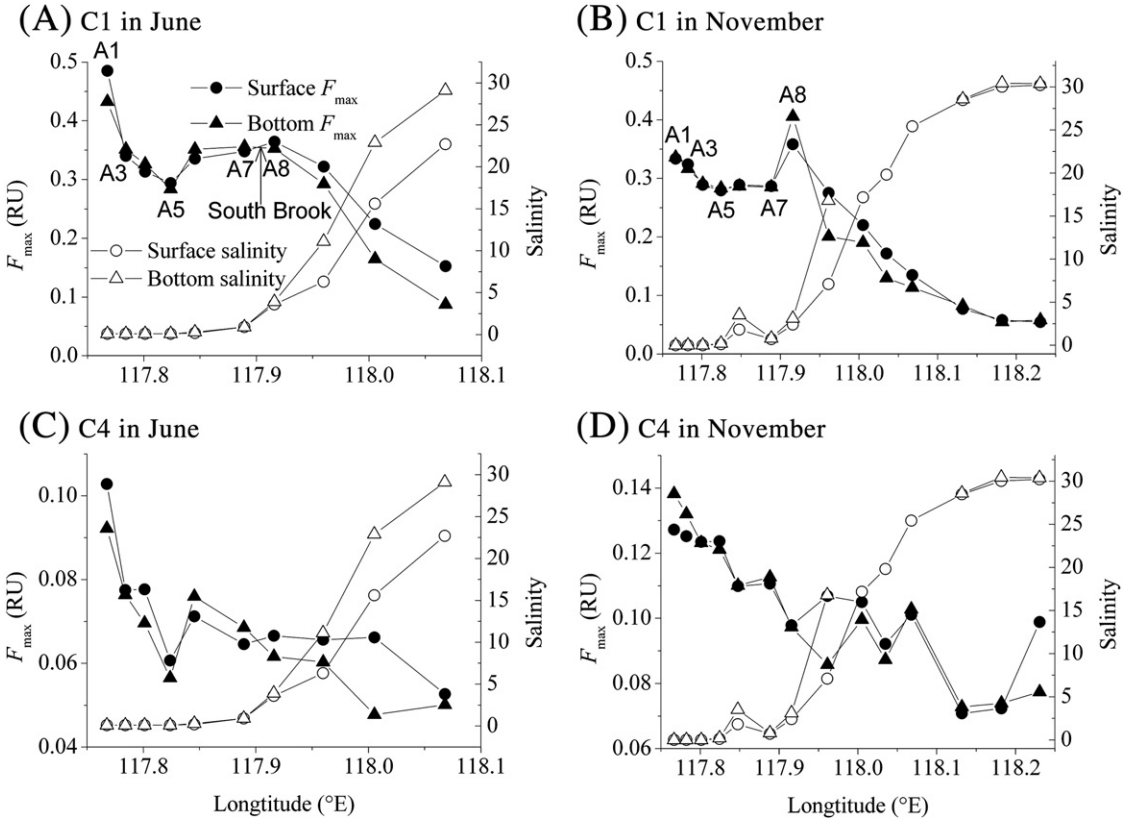

Fig. 5. Spatial distribution of C1 and C4 in selected months for the sections of A1-A3~A9-J6-J1 in June and A1-A3~A9-J6-J5-J1-KM2~KM4 in November, refer to graph A for the corresponding parameters to different symbols. South Brook enters the estuary at 117.902°E (i.e., between A7 and A8).

similar removal and addition processes as seen for the fluorescent components. On the contrary, DOC generally decreased with increasing salinity in the middle and high salinity zone, indicating the dominance of water mixing, although some stations were also influenced by addition/removal processes during some cruises.

The values of TDN were 0.11 mg L^{-1} to 4.30 mg L^{-1} (Fig. 6B). Except for those values at the river–estuary interface, TDN decreased linearly with salinity, indicating that it was quite conservative in the Jiulong Estuary. Although the dissolved inorganic nitrogen can be utilized by phytoplankton, this process did not impact notably the overall linear mixing line of TDN. The conservative mixing of TDN also indicated that there was no significant source of nitrogen in the estuary. These results could be explained by the large supply of TDN from fluvial discharge (Fig. 6B) and the rapid estuarine mixing which was the dominant process controlling the distribution of water constituents.

3.3. Processes of fluorescent components in Jiulong Estuary interfaces

3.3.1. River–estuary interface

North Brook and South Brook converge at the river–estuary interface. They flow through two sub-watersheds with different land use/land cover patterns and human disturbances. This interface is also characterized by a high turbidity (e.g., Yang and Hu, 1997). They make the behavior of the identified components rather complicated at this interface (Fig. 5). Freshwater dominated a large area and F_{max} of the individual components decreased in the upper estuary. For instance, salinity was constantly low (0.1) in June from the river end downstream to 117.82°E (station A5), while F_{max} of C1 and C4 decreased significantly (Fig. 5A, C). Station A1 was located in the West Brook while A3 was at the convergent point of the West Brook and the North Brook. Thus, the rapid decrease in the fluorescent intensity from A1 to A3 apparent in Fig. 5 was at least partly due to the mixing of the water from those two tributaries with different CDOM contents. For example, F_{max} of C1 and C4 in the lower part of the North Brook (0.15 RU and 0.05 RU) were much lower than those in the West Brook (0.33 RU and 0.13 RU) in November. Further decrease of the fluorescent intensity downstream while salinity remained constant was probably due to some removal processes (e.g., adsorption at this turbid zone). Previous studies have revealed the importance of adsorption in the removal of CDOM in turbid estuaries (Uher et al., 2001; Spencer et al., 2007). Guo et al. (2007) also find the removal of CDOM in the low salinity zone of Jiulong Estuary during some cruises based absorption results. Our results demonstrated that the removal might exist over a larger spatial scale in the river–estuary interface.

3.3.2. Estuary–coastal interface

Dynamics of DOM showed a significant variation at the mouth of the estuary, as is demonstrated by the covariate analysis (Fig. 4). The regression line between log (C4) and log (C1) showed a sharp transition at the salinity of 30 (Fig. 4C). Similar transition was observed for the relationship between log (C2) and log (C1) (although much smaller) (Fig. 4A). Such a division separated samples within the estuarine mouth and those from coastal ocean. This was also supported by the transition of other chemical parameters in this area (e.g., TDN in November; Fig. 6B). This indicated that there was a decoupling between the behaviors of C1, C3 and that of C2, C4 across this interface and there should be another source of CDOM with a different composition in coastal water, which should be derived from Minzhe Coastal Current along the western Taiwan Strait.

3.4. Temporal variation of DOC and the fluorescent components

Temporal variations of DOC and F_{max} of C(1–4) in freshwater and seawater endmembers are shown in Fig. 7. The seawater endmember was only available for November and June, because the investigations

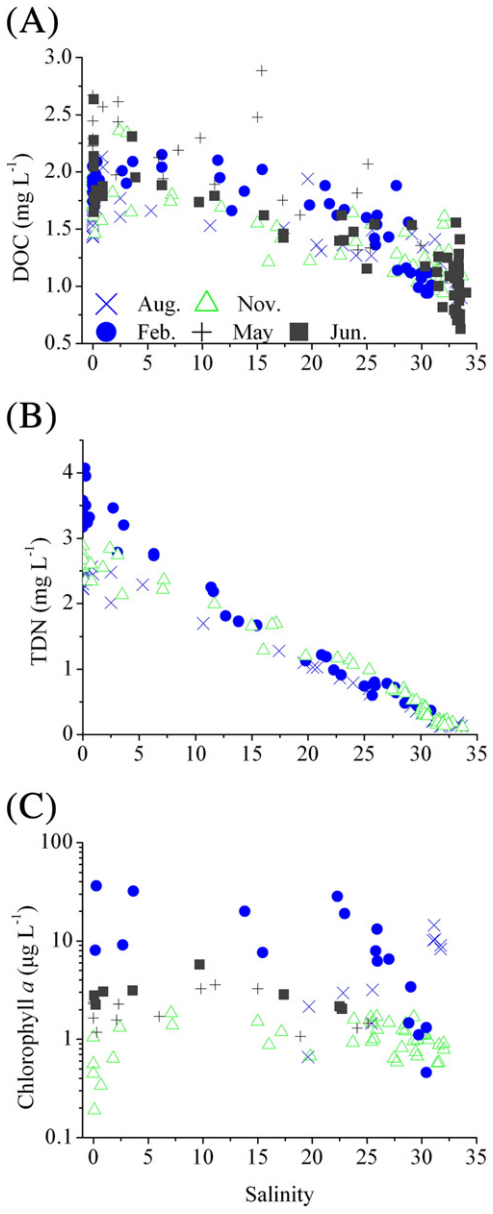

Fig. 6. Spatial and temporal variation of DOC, TDN and chlorophyll *a*.

did not extend to the coast in other months. DOC was higher in February and May than those in other months within the estuary (Fig. 6A), likely due to different mechanisms. In February, DOC in freshwater was not elevated (Fig. 7A) and the higher concentration in the estuary was likely due to higher in situ primary production. In contrast, freshwater DOC in May was highest among the five cruises (Fig. 7A), suggesting that the increased freshwater DOC input could explain largely the higher estuarine DOC.

All the fluorescent components were an order of magnitude more abundant in freshwater than in seawater. Therefore, the small variation in seawater endmember is not expected to significantly affect the variation in the estuary. This is similar to the results based on absorption measurements (Guo et al., 2007).

The tryptophan-like C4 had an evident seasonal variation from the freshwater endmember (Fig. 7B) to the middle salinity zone of the estuary (Fig. 3D), with higher F_{max} in February and November. Hence, C4 (and also its percent in the total fluorescence) was more abundant in the dry season, likely indicating an increased autochthonous production in both the freshwater and the estuary. This is supported by the much higher chlorophyll *a* concentration in February than any other months for samples with salinity<27.5 (Fig. 6C), maybe associated with elevated nutrient concentration. For example, TDN was highest in February in the low salinity zone (S<10, Fig. 6B). Chlorophyll *a* and TDN were not high in November, and the elevated tryptophan-like level could be explained by either the degradation of algal materials or the increased protein-like level in the river (Hong et al., in press) although the freshwater discharge decreased in the dry season. These results were supported by the fact that the chlorophyll *a* concentration was correlated significantly with F_{max} of the tryptophan-like C4 but not those of other fluorescent components (Table 2). There was also a weak but significant correlation between the chlorophyll *a* concentration and TDN ($r=0.390$, $p<0.001$). However, TDN was correlated more strongly with F_{max} of C(1–3) than that of C4 (Table 2), since TDN and C(1–3) were all largely derived from the fluvial discharge while C4 received significant additions from the autochthonous production in the estuary.

In contrast, C3, which had longest excitation and emission wavelengths and was likely a terrestrial humic-like component, was

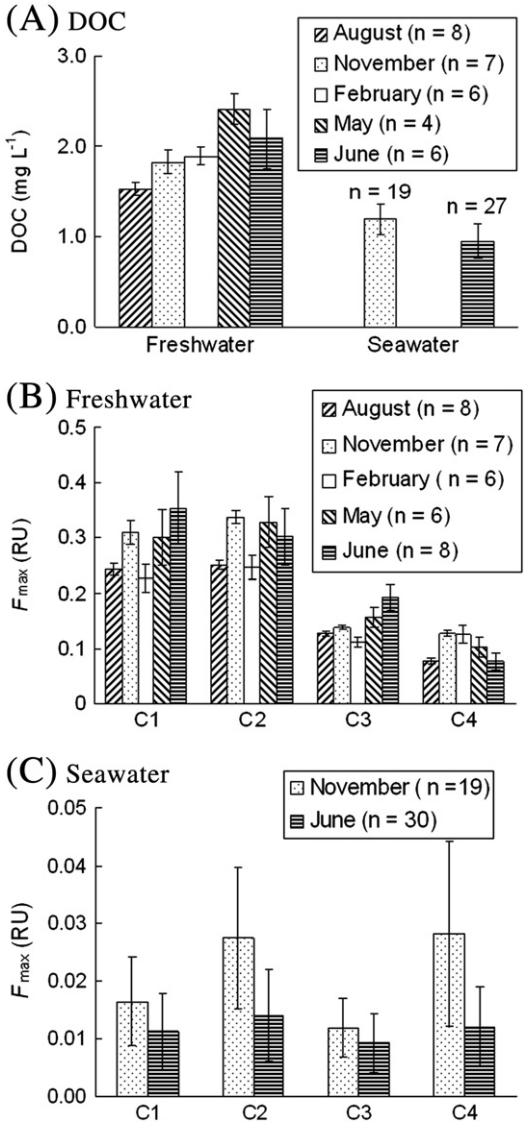

Fig. 7. Temporal variation of DOC and F_{max} of C(1–4) in freshwater and seawater endmembers. The freshwater endmember was represented as the mean DOC or F_{max} of samples at salinity 0, while the seawater one as that from coastal ocean in November and June (i.e., stations in Fig. 1B). The sample numbers were also shown in brackets except that those for marine DOC were shown above the bars. The error bars equaled to ±1 standard error.

Table 2
Correlation coefficient (r) between TDN, chlorophyll a concentration (Chl a) and F_{max} (RU) of the fluorescent components.

	Chl a ($n=103$)	TDN ($n=171$)
C1	0.048	0.87**
C2	0.056	0.86**
C3	0.067	0.84**
C4	0.36**	0.61**

**Correlation is significant at the 0.01 level (two-tailed).

most abundant in June while most depleted in February (Fig. 7B and Fig. 3C). This agreed with the higher freshwater discharge in the wet season than in the dry season. The seasonal variation of C1 was similar to C3 (Fig. 3A and Fig. 7B), considering the strong correlation between them (Fig. 4B). However, higher levels of C1 were also found in November in the freshwater endmember, likely due to other addition processes (Fig. 7B). The seasonal variation of C2 was not clear in the estuary (i.e., highest in November and lowest in February, Fig. 3B) but similar to C1 in freshwater (Fig. 7B). As mentioned above, C2 was more likely protein-like and was largely derived from fluvial input. Hence, the seasonal variation of C2 in the estuary was affected by the variations of both the freshwater primary production and the freshwater discharge.

3.5. Tracing DOC using fluorescence measurements

It is only recently that the relationships between DOC and fluorescent components identified by PARAFAC were examined (Kowalczuk et al., 2010), although it is important to determine which component correlates with DOC closely and which range of excitation and emission wavelengths is suitable for tracing DOC. In addition, the seasonal variability of the correlations is still not clear.

In this study, DOC can be retrieved roughly from the fluorescence intensity of C(1–3) (Table 3). However, temporal variation of the retrieving algorithm was also observed. While the correlations between DOC and F_{max} of the four components in August and November were largely similar, those in February and May seemed to be distinct. The higher slopes in the later 2 months indicated fewer contributions from fluorescent components to DOC and/or lower fluorescent quantum yield of DOM. Although the variation of different source intensities and maybe some other processes like photobleaching might affect the retrieving algorithm, this study suggested that the fluorescence at excitation and emission wavelength of C1 (or C2 and C3) were most suitable to trace DOC.

Multi linear regressions with more than one component as independent variables were also tested but not found to improve the relationship enough. For example, a multi-linear regression, taking DOC as the dependent variable and all the components as independent variables, only yielded a little better results ($r=0.84$, data not shown) than linear regressions of DOC vs. C(1–3) ($r=0.82$–0.83, Table 3).

Table 3
Correlations between DOC (y, mg L^{-1}) and F_{max} (RU) of the components identified.

Component F_{max} (x)	Cruise	Sample size (n)	Correlation coefficient (r)	Regression equation
C1	all	245	0.82	$y=1.03+3.2x$
	August 2008	36	0.84	$y=1.02+2.51x$
	November 2008	71	0.86	$y=1.04+2.49x$
	February 2009	64	0.87	$y=1.01+4.27x$
	May 2009	23	0.69	$y=1.28+3.72x$
	June 2009	51	0.93	$y=0.93+3.05x$
C2	all	245	0.83	$y=0.96+3.32x$
	August 2008	36	0.84	$y=0.95+2.74x$
	November 2008	71	0.84	$y=1.01+2.25x$
	February 2009	64	0.88	$y=0.92+4.15x$
	May 2009	23	0.69	$y=1.16+3.70x$
	June 2009	51	0.93	$y=0.90+3.58x$
C3	all	245	0.82	$y=0.98+6.37x$
	August 2008	36	0.85	$y=0.97+5.12x$
	November 2008	71	0.83	$y=1.01+5.12x$
	February 2009	64	0.89	$y=0.83+9.76x$
	May 2009	23	0.70	$y=1.09+8.08x$
	June 2009	51	0.92	$y=0.90+5.54x$
C4	all	245	0.61	$y=0.96+7.30x$
	August 2008	36	0.56	$y=1.03+6.12x$
	November 2008	71	0.56	$y=0.97+5.17x$
	February 2009	64	0.80	$y=0.10+14.47x$
	May 2009	23	0.47	$y=1.16+11.24x$
	June 2009	51	0.91	$y=0.75+16.10x$

4. Conclusions

This study demonstrated the distinct behaviors of different fluorescent components in the Jiulong Estuary and the significance of CDOM dynamics in the watershed–estuary interface and the estuary–coastal interface. CDOM originated from several sources in the Jiulong Estuary (i.e., terrigenous/fluvial input, autochthonous production, coastal currents and likely from the surrounding mangrove and the resuspended sediments). CDOM can be rather non-conservative in the upper estuary (i.e., being removed rapidly in the uppermost estuary and then receiving significant addition from the South Brook and a series of other sources including the releasing from particles and the adjacent mangrove wetlands). Autochthonous dissolved organic matter (as indicated by the tryptophan-like component) received significant addition over a wide range of salinity within the estuary, but decreased more rapidly in the coastal region. Therefore, riverine DOM may have undergone significant removal and/or addition in the estuarine environment before being transported finally to the ocean. This should be considered in evaluating the land-ocean DOM flux as well as understanding the reactivity of DOM that finally reaches the ocean.

The seasonal variations of different components were also different, likely associated with the different temporal variability of their sources. The protein-like C4 was most abundant in February in the dry season, likely due to the increased autochthonous productivity. In contrast, the humic-like C1 and C3 were much more abundant in June than in February, likely due to the seasonal variability of fluvial discharge. These would lead to the seasonal variation of the chemical composition (i.e., the percent of protein-like materials) and hence the bioavailability of DOM in the estuary. Therefore, the different mixing behavior and seasonal variations of different DOM components should be studied further by using biomarkers like lignin, amino acids and carbohydrates in order to understand the biogeochemical role of DOM in the estuarine environments.

Acknowledgements

This work was funded by the National Natural Science Foundation of China (40810069004, 40776041 and 40676046), National High Technology Research and Development Program of China (2007AA091704) and the Program for New Century Excellent Talents (NCET) for Weidong Guo. We thank the captain and crew of *R/V* Yanping II and *R/V* Ocean I. We also thank Zhuo Jianfu, Yan Yuchao, Huang Shuyuan and Ye Xiaoyu for their assistances in sample collection and measurements. Dr. Wang Xinhong, Chen Zhaozhang, Sun Zhenyu and Zhu Jia are appreciated for sharing PAHs and salinity data. We thank Dr. Huang Bangqin for help in chlorophyll measurements and Dr. Zhai Weidong for his comments and revision suggestions. We thank Professor John Hodgkiss for his help with English. The anonymous reviewers are thanked for their comments that greatly improved the quality of the paper.

References

Abril, G., Nogueira, M., Etcheber, H., Cabecadas, G., Lemaire, E., Brogueira, M.J., 2002. Behaviour of organic carbon in nine contrasting European estuaries. Estuarine Coastal and Shelf Science 54, 241–262.

Andersson, C.A., Bro, R., 2000. The N-way Toolbox for MATLAB. Chemometrics Intelligent Laboratory System 52, 1–4.

Baker, A., 2001. Fluorescence excitation-emission matrix characterization of some sewage-impacted rivers. Environmental Science and Technology 35, 948–953.

Bushaw, K.L., Zepp, R.G., Tarr, M.A., Schulz-Jander, D., Bourbonniere, R.A., Hodson, R.E., Miller, W.L., Bronk, D.A., Moran, M.A., 1996. Photochemical release of biologically available nitrogen from aquatic dissolved organic matter. Nature 381, 404–407.

Chen, S.T., Ruan, W.Q., Zhang, L.P., 1985. Chemical characteristics of nutrient ellments in the Jiulong Estuary and the calculation of its flux. Tropical Oceanology 4, 16–24 (in Chinese with English abstract).

Cheng, Y.Y., Guo, W.D., Xia, E.Q., Hu, M.H., 2008. Fluorescence characteristics of chromophoric dissolved organic matter and its distribution in sediment pore waters from Xiamen Bay. Oceanography in Taiwan Straits 27, 8–14 (in Chinese with English abstract).

Coble, P.G., 1996. Characterization of marine and terrestrial DOM in seawater using excitation-emission matrix spectroscopy. Marine Chemistry 51, 325–346.

Coble, P.G., 2007. Marine optical biogeochemistry: the chemistry of ocean color. Chemical Review 107, 402–418.

Coble, P.G., Del Castillo, C.E., Avril, B., 1998. Distribution and optical properties of CDOM in the Arabian Sea during the 1995 Southwest Monsoon. Deep-Sea Research II 45, 2195–2223.

Cory, R.M., McKnight, D.M., 2005. Fluorescence spectroscopy reveals ubiquitous presence of oxidized and reduced quinones in dissolved organic matter. Environmental Science and Technology 39, 8142–8149.

Fellman, J.B., Spencer, R.G.M., Hernes, P.J., Edwards, R.T., D'Amore, D.V., Hood, E., 2010. The impact of glacier runoff on the biodegradability and biochemical composition of terrigenous dissolved organic matter in near-shore marine ecosystems. Marine Chemistry 121, 112–122.

Foden, J., Sivyer, D.B., Mills, D.K., Devlin, M.J., 2008. Spatial and temporal distribution of chromophoric dissolved organic matter (CDOM) fluorescence and its contribution to light attenuation in UK waterbodies. Estuarine Coastal and Shelf Science 79, 707–717.

Gors, S., Rentsch, D., Schiewer, U., Karsten, U., Schumann, R., 2007. Dissolved organic matter along the eutrophication gradient of the Dar beta-Zingst Bodden Chain, Southern Baltic Sea: I. Chemical characterisation and composition. Marine Chemistry 104, 125–142.

Guo, W.D., Stedmon, C.A., Han, Y.C., Wu, F., Yu, X.X., Hu, M.H., 2007. The conservative and non-conservative behavior of chromophoric dissolved organic matter in Chinese estuarine waters. Marine Chemistry 107, 357–366.

Han, Y.C., Guo, W.D., 2008. Factors influencing analysis analysis of chromophoric dissolved organic matter in estuarine waters by excitation emission fluorescence matrix spectroscopy (EEMS). Acta Scientiae Circumstaniae 28, 1646–1653 (in Chinese with English abstract).

Hansell, D., Carlson, C. (Eds.), 2002. Biogeochemistry of Marine Dissolved Organic Matter. Academic Press, NewYork, pp. 509–578.

He, B.Y., Dai, M.H., Zhai, W.D., Wang, L.F., Wang, K.J., Chen, J.H., Lin, J.R., Han, A.G., Xu, Y.P., 2010. Distribution, degradation and dynamics of dissolved organic carbon and its major compound classes in the Pearl River estuary, China. Marine Chemistry 119, 52–64.

Hong, H.S., Cao, W.Z., 2000. Budgets for estuaries in China: Jiulong River Estuary: LOICZ reports, 16, pp. 47–52.

Hong, H.S., Wu, J.Y., Shang, S.L., Hu, C.M., 2005. Absorption and fluorescence of chromophoric dissolved organic matter in the Pearl River Estuary, South China. Marine Chemistry 97, 78–89.

Hong, H.S, Yang, L.Y., Guo, W.D., Wang, F.L., Yu, X.X., in press. Characterization of dissolved organic matter under contrasting hydrologic regimes in a subtropical watershed using PARAFAC model. Biogeochemistry.

Jaffé, R., Boyer, J.N., Lu, X., Maie, N., Yang, C., Scully, N.M., Mock, S., 2004. Source characterization of dissolved organic matter in a subtropical mangrove-dominated estuary by fluorescence analysis. Marine Chemistry 84, 195–210.

Kieber, R.J., Zhou, X., Mopper, K., 1990. Formation of carbonyl compounds from UV-induced photodegradation of humic substances in natural waters: fate of riverine carbon in the sea. Limnology and Oceanography 35, 1503–1515.

Kowalczuk, P., Durako, M.J., Young, H., Kahn, A.E., Cooper, W.J., Gonsior, M., 2009. Characterization of dissolved organic matter fluorescence in the South Atlantic Bight with use of PARAFAC model: Interannual variability. Marine Chemistry 113, 182–196.

Kowalczuk, P., Cooper, W.J., Durako, M.J., Kahn, A.E., Gonsior, M., Young, H., 2010. Characterization of dissolved organic matter fluorescence in the South Atlantic Bight with use of PARAFAC model: Relationships between fluorescence and its components, absorption coefficients and organic carbon concentrations. Marine Chemistry 118, 22–36.

Lawaetz, A.J., Stedmon, C.A., 2009. Fluorescence intensity calibration using the Raman scatter peak of water. Applied Spectroscopy 63, 936–940.

Moran, M.A., Zepp, R.G., 1997. Role of photoreactions in the formation of biologically labile compounds from dissolved organic matter. Limnology and Oceanography 42, 1307–1316.

Murphy, K.R., Ruiz, G.M., Dunsmuir, W.T.M., Waite, T.D., 2006. Optimized parameters for fluorescence-based verification of ballast water exchange by ships. Environmental Science and Technology 40, 2357–2362.

Ou, L.J., Huang, B.Q., Lin, L.Z., Hong, H.S., Zhang, F., Chen, Z.Z., 2006. Phosphorus stress of phytoplankton in the Taiwan Strait determined by bulk and single-cell alkaline phosphatase activity assays. Marine Ecology-Progress Series 327, 95–106.

Shank, G.C., Lee, R., Vähätalo, A., Zepp, R.G., Bartels, E., 2010. Production of chromophoric dissolved organic matter from mangrove leaf litter and floating Sargassum colonies. Marine Chemistry 119, 172–181.

Sharp, J.H., Yoshiyama, K., Parker, A.E., Schwartz, M.C., Curless, S.E., Beauregard, A.Y., Ossolinski, J.E., Davis, A.R., 2009. A biogeochemical view of estuarine eutrophication: seasonal and spatial trends and correlations in the delaware estuary. Estuaries and Coasts 32, 1023–1043.

Spencer, R.G.M., Ahad, J.M.E., Baker, A., Cowie, G.L., Ganeshram, R., Upstill-Goddard, R.C., Uher, G., 2007. The estuarine mixing behaviour of peatland derived dissolved organic carbon and its relationship to chromophoric dissolved organic matter in two North Sea estuaries (U.K.). Estuarine Coastal and Shelf Science 74, 131–144.

Spencer, R.G.M., Aiken, G.R., Butler, K.D., Dornblaser, M.M., Striegl, R.G., Hernes, P.J., 2009. Utilizing chromophoric dissolved organic matter measurements to derive export and reactivity of dissolved organic carbon exported to the Arctic Ocean: A case study of the Yukon River, Alaska. Geophysical Research Letters 36, L06401. doi:10.1029/2008GL036831.

Stedmon, C.A., Bro, R., 2008. Characterizing dissolved organic matter fluorescence with parallel factor analysis: a tutorial. Limnology and Oceanography- Methods 6, 572–579.

Stedmon, C.A., Markager, S., 2005. Resolving the variability in dissolved organic matter fluorescence in a temperate estuary and its catchment using PARAFAC analysis. Limnology and Oceanography 50, 686–697.

Stedmon, C.A., Markager, S., Bro, R., 2003. Tracing dissolved organic matter in aquatic environments using a new approach to fluorescence spectroscopy. Marine Chemistry 82, 239–254.

Uher, G., Hughes, C., Henry, G., Upstill-Goddard, R.C., 2001. Non-conservative mixing behavior of colored dissolved organic matter in a humic-rich, turbid estuary. Geophysical Research Letters 28, 3309–3312.

Wu, Y., Zhang, J., Liu, S.M., Zhang, Z.F., Yao, Q.Z., Hong, G.H., Cooper, L., 2007. Sources and distribution of carbon within the Yangtze River system. Estuarine Coastal and Shelf Science 71, 13–25.

Yamashita, Y., Jaffé, R., 2008. Characterizing the interactions between trace metals and dissolved organic matter using excitation−emission matrix and parallel factor analysis. Environmental Science and Technology 42, 7374–7379.

Yamashita, Y., Tanoue, E., 2003. Chemical characterization of protein-like fluorophores in DOM in relation to aromatic amino acids. Marine Chemistry 82, 255–271.

Yamashita, Y., Jaffé, R., Maie, N., Tanoue, E., 2008. Assessing the dynamics of dissolved organic matter (DOM) in coastal environments by excitation emission matrix fluorescence and parallel factor analysis (EEM-PARAFAC). Limnology and Oceanography 53, 1900–1908.

Yang, Y.P., Hu, M.H., 1997. The geochemistry of Jiulong River Estuary. In: Zhang, J. (Ed.), The biogeochemistry of major chinese estuaries-transport of chemical materials and environment. Ocean Press, Beijing, pp. 54–67.

Zepp, R.G., Shank, G.C., Stabenau, E., Patterson, K.W., Cyterski, M., Fisher, W., Bartels, E., Anderson, S.L., 2008. Spatial and temporal variability of solar ultraviolet exposure of coral assemblages in the Florida Keys: Importance of colored dissolved organic matter. Limnology and Oceanography 53, 1909–1922.